Splitting Water on Metal Oxide Surfaces

ARTICLE *in* THE JOURNAL OF PHYSICAL CHEMISTRY C · SEPTEMBER 2011

Impact Factor: 4.77 · DOI: 10.1021/jp2032884

7 AUTHORS, INCLUDING:

Hu Xu
South University of Science and Technology …
41 PUBLICATIONS **415** CITATIONS
SEE PROFILE

Rui Qin Zhang
City University of Hong Kong
326 PUBLICATIONS **5,690** CITATIONS
SEE PROFILE

S. Y. Tong
South University of Science and Technology …
285 PUBLICATIONS **7,326** CITATIONS
SEE PROFILE

THE JOURNAL OF PHYSICAL CHEMISTRY C

ARTICLE

pubs.acs.org/JPCC

Splitting Water on Metal Oxide Surfaces

Hu Xu,[†] Rui Qin Zhang,[‡] Alan M. C. Ng,[†,§] Aleksandra B. Djurišić,[§] Hung Tat Chan,[∥] Wai Kin Chan,[∥] and S. Y. Tong*[,†]

[†]Nanostructure Institute for Energy and Environmental Research, Division of Physical Sciences, South University of Science and Technology of China, Shenzhen, China

[‡]Department of Physics and Materials Science, City University of Hong Kong, Tat Chee Avenue, Kowloon, Hong Kong

[§]Department of Physics, The University of Hong Kong, Pokfulam Road, Hong Kong

[∥]Department of Chemistry, The University of Hong Kong, Pokfulam Road, Hong Kong

Supporting Information

ABSTRACT: We have identified a class of metal oxide surfaces that are very effective in dissociating water. These oxide surfaces are characterized by having their surface O 2p level lying significantly above the valence band maximum (VBM) and within the band gap. Density functional theory is used to determine the adsorption energy per water molecule and finds that water dissociates completely at all coverages on these surfaces. Fourier transform infrared (FTIR) spectroscopy is used to verify that there is little or no molecular water present on the surface. Besides splitting water, this class of metal oxide surfaces should also be effective in splitting other kinds of hydrogen compounds. By contrast, oxides whose surface O 2p level lies buried inside the valence band are much less reactive, and water adsorbs on these surfaces in molecular form.

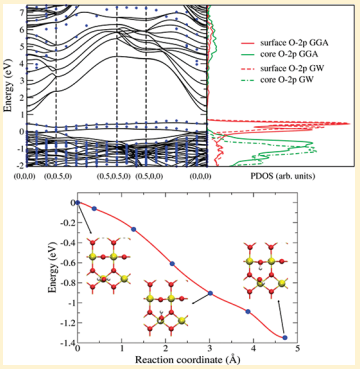

1. INTRODUCTION

Metal oxides have many technologically important applications, as they are used in new-generation photocatalysts, antibacterial agents, and solid-state sensors.[1−4] As photocatalysis and electrochemistry experiments always involve the presence of water, the understanding of how water interacts with metal oxide surfaces is of fundamental interest and importance.[5,6] Studies have shown that, while water adsorbs molecularly on some oxide surfaces, it completely dissociates on other oxide surfaces.[7−19] The cause for water splitting on metal oxide surfaces is not completely understood.

In this article, we report convincing data of a class of metal oxide surfaces that effectively splits water on their surfaces at all coverages. This study, based on theoretical calculations and experimental measurements, focuses on the behavior of water on three metal oxide surfaces: $SnO_2(110)$, $In_2O_3(110)$, and r-$TiO_2(110)$. The results show that an important factor that affects water splitting on the surface is the position of the surface O 2p level relative to the top of the valence band. For a stoichiometric oxide surface, the 2p levels of surface and bulk oxygen occupy the upper parts of the valence band. If the surface O 2p level of the bare surface lies high above the valence band maximum (VBM; i.e., well inside the gap), as in $SnO_2(110)$ and $In_2O_3(110)$, then these oxide surfaces are very effective water splitters. Besides $SnO_2(110)$ and $In_2O_3(110)$, we have identified other metal oxide surfaces also belonging to this class.[20] In contrast, if the surface O 2p level is buried inside the valence band, as in r-$TiO_2(110)$, then this surface is much less reactive to water and water molecules tend to adsorb without dissociation. In the following, we shall present the theoretical and experimental findings, elucidate the cause of the observed effect, and discuss the implications on other hydrogen compounds.

2. COMPUTATIONAL AND EXPERIMENTAL DETAILS

The calculations are based on DFT using the Vienna ab initio simulation package (VASP).[21,22] The projected augmented wave (PAW) potential[23] is generated taking scalar relativistic corrections into account. The Ti, Sn, and In atoms are described by 10 valence electrons ($3p^6 4s^2 3d^2$), 14 valence electrons ($4d^{10} 5s^2 5p^2$), and 13 valence electrons ($4d^{10} 5s^2 5p^1$), respectively. The Perdew and Wang (PW91)[24] functional is used as it gives accurate descriptions of the hydrogen bonds.[25] A cutoff energy of 450 eV and Monkhorst−Pack[26] samplings are applied. All oxide surfaces are separated by a vacuum region of 10 Å to avoid image interaction, and the conjugate gradient method is used to optimize atomic coordinates until the Hellmann−Feynman forces on each atom are smaller than 0.02 eV/Å. The energy barriers and pathways are calculated using the nudged elastic band (NEB) method.[27]

Received: April 8, 2011
Revised: July 26, 2011
Published: August 29, 2011

As density functional theory/generalized gradient approximation (DFT-GGA) calculations typically underestimate the band gap, the GW correction[28] is applied at selected points of the BZ. Generally, GGA and GW results agree well for filled states, while the GW calculations provide a better description of unoccupied states and give more accurate values for the band gap. For example, GW calculated band gaps for SnO_2 and *r*-TiO_2 bulk crystals are respectively 3.12 and 3.65 eV in reasonably good agreement with experimentally measured bulk gaps of 3.6 eV (SnO_2) and 3.0 eV (*r*-TiO_2). For the experiments using Fourier transform infrared (FTIR), a mixture containing 12 mg of oxide nanoparticles (all nanoparticles were purchased from Nanostructured & Amorphous Materials, Inc.) with 250 mg of infrared-grade KBr (99+%, International Laboratory, U.S.A.) is used and pressed into pellets. The FTIR measurements were performed using the Shimadzu FTIR-8300 FTIR spectrophotometer.

3. RESULTS AND DISCUSSION

Metal oxides possess a wide range of geometric forms with different coordination numbers for the metal and oxygen ions. To study the electronic structure and water adsorption behavior, we present results of theoretical calculations and experimental measurements on three representative metal oxide surfaces: *r*-TiO_2-(110), SnO_2(110), and In_2O_3(110). The (110) surfaces are selected because they are the most stable facets due to their low surface energies, and nanoparticles are primarily composed of these most stable surfaces derived from Wulff construction by minimizing surface energies.

In Figure 1, we show the band structure and projected density of states (PDOS) for three stoichiometric oxide surfaces. Dots and broken lines denote GW results. In Figure 1a, for the bare SnO_2(110) surface, the surface O 2p level has two significant bands above the VBM. The upper (major) band is inside the gap and 0.70 eV above the VBM at Γ. The lower (minor) band is also inside the gap, but it touches the VBM at Γ. The center of gravity (cog) of the surface O 2p level is 0.59 eV above the VBM. The situation for In_2O_3(110), shown in Figure 1b, is similar, with the surface O 2p level appearing as tightly bunched bands in the gap, and its cog is 0.38 eV above the VBM. By contrast, *r*-TiO_2(110), which shares the same geometric structure as SnO_2(110), exhibits very different surface O 2p bands relative to its VBM. As Figure 1c shows, there is no surface band in the gap, and the surface O 2p level appears as a broad band within the valence band of the core O 2p level. The cog of the surface O 2p level is 0.49 eV *below* the VBM. As we shall show, the difference in the location of the surface O 2p level relative to the VBM has a strong effect on water splitting on the surface. In passing, we see from Figure 1 that there are large upshifts of the unoccupied states (conduction bands) in the GW results compared to the DFT-GGA results, bringing the calculated band gaps in closer agreement with experimental values. However, GW calculations are not carried out for In_2O_3-(110) because of the very large computational requirement for that surface. As the effect discussed here involves only occupied levels and the difference between GW and DFT-GGA for filled levels are small as evidenced in the results of SnO_2(110) and *r*-TiO_2(110), the conclusions we draw are not affected by skipping GW calculations for In_2O_3(110).

Water adsorption at different coverages on the three oxide surfaces is considered. The adsorption energies per water molecule for molecular, dissociated, and mixed states are compared for different water adsorption configurations, and the structure

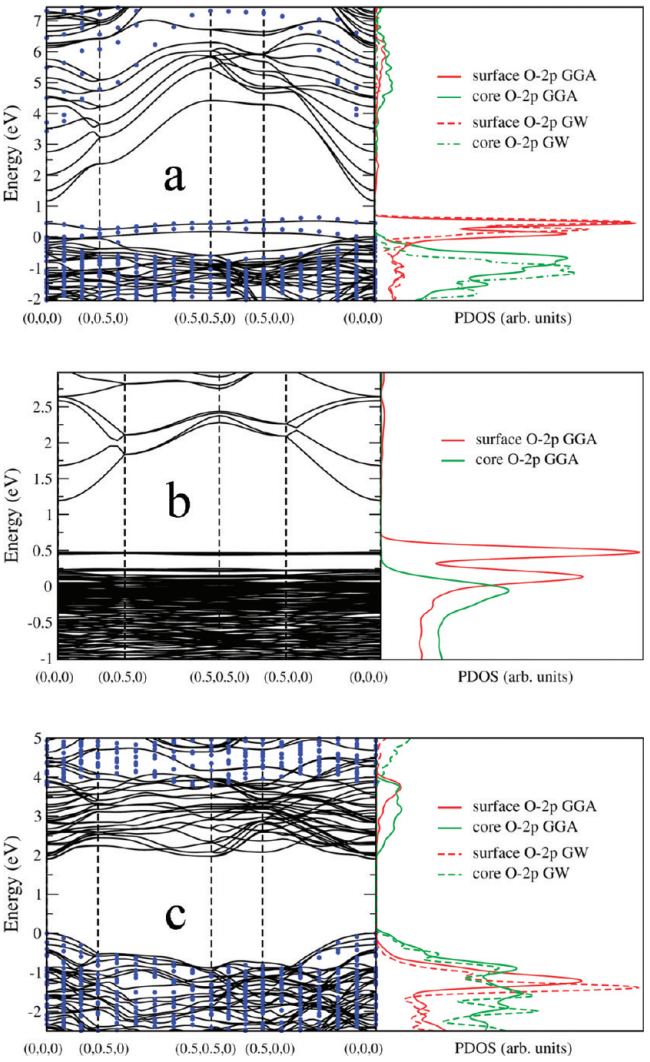

Figure 1. Electronic structure and PDOS of bare (a) SnO_2(110) surface, (b) In_2O_3(110) surface, and (c) *r*-TiO_2(110) surface. Solid lines: DFT-GGA; dots and broken lines: GW. The top of bulk valence bands at Γ for DFT-GGA and GW results are set at zero.

with the lowest energy is obtained. Table 1 summarizes the calculated results. On SnO_2(110), water adsorbs in completely dissociated form at all three coverages considered: i.e., 0.25, 0.5, and 1.0 ML, respectively. The binding energy of dissociated water is large, on the order of −1.5 eV per molecule, in agreement with results of other calculations.[15] The bond length between O of the dissociated OH and surface Sn (d_{O-Sn}) is 2.06 Å at 1.0 ML coverage, slightly shorter than the bulk O−Sn bond (2.07 Å). Water binding in molecular form is unstable on this surface with near zero barriers for dissociation (Figure 2a). A similar trend is observed on In_2O_3(110), with dissociated adsorption favored at all 0.125, 0.25, 0.5, and 1.0 ML coverages considered, and the binding energy is also large, between −1.08 to −1.26 eV per water molecule. Molecular adsorption is stable only at the lowest coverage, i.e., at 0.125 ML, but even here, the reactive barrier going from molecular form to dissociative form is close to zero (less than 0.01 eV, Figure 2b) and dissociated adsorption is favored over molecular adsorption by over 0.43 eV per molecule. At this coverage, the bond length between O of the adsorbed molecular water and surface In (m_{O-In}) is 2.27 Å, and that for dissociative

dx.doi.org/10.1021/jp2032884 |J. Phys. Chem. C 2011, 115, 19710–19715

water (d_{O-In}) is 2.04 Å, while the average bulk bond length in In_2O_3 is 2.22 Å. At higher coverages, only dissociated adsorption is stable, and d_{O-In} is 2.06 Å at 1 ML. The situation is qualitatively different on *r*-TiO_2(110). Three points are worth noting. First, molecular adsorption is the most stable configuration for all eight coverages considered. Second, the binding energy per water molecule is much smaller compared to that on SnO_2(110) and In_2O_3-(110), averaging only about −0.8 eV per water molecule in good agreement with previous results.[29] Third, the energy difference between different forms of adsorption is small, being only 0.107 eV at 0.083 ML (between molecular and dissociated forms) and 0.113 eV at 1.0 ML (between molecular and mixed forms). The bond length between O of the adsorbed water and surface Ti in dissociative adsorption (d_{O-Ti}) and that in molecular adsorption (m_{O-Ti}) are respectively shorter and longer than the average bulk bond length of O−Ti (1.98 Å). Also, m_{O-Ti} increases from 2.24 Å at 0.083 ML to 2.34 Å at 1 ML, while d_{O-Ti} also increases from 1.84 Å to 1.93 Å at these coverages. However, different from SnO_2(110) and In_2O_3(110) surfaces, the reactive barrier for water dissociation on *r*-TiO_2(110) can be quite large, about 0.38 eV per water molecule (Figure 2c).

Table 1. Adsorption Energy Δ (in eV) Per Water Molecule on Oxide Surfaces at Different Coverages *θ*[a]

surface	θ	unit cell	Δ_{H_2O}	Δ_{H-OH}	Δ_{Mixed}	m_{O-M}	d_{O-M}
SnO_2(110)	0.25	p(2 × 2)		−1.560			2.05
	0.50	p(2 × 1)		−1.515			2.05
	1.00	p(1 × 1)		−1.532			2.06
r-TiO_2(110)	0.083	p(6 × 2)	−0.783	−0.676		2.24	1.84
	0.125	p(4 × 2)	−0.756	−0.618		2.25	1.84
	0.25	p(2 × 2)	−0.708	−0.420		2.27	1.88
	0.25	p(1 × 4)	−0.827	−0.509		2.32	1.93
	0.333	p(1 × 3)	−0.822	−0.500		2.32	1.93
	0.50	p(1 × 2)	−0.818	−0.488		2.32	1.93
	0.50	p(2 × 1)	−0.688	−0.417		2.28	1.89
	1.00	p(2 × 1)	NA	NA	−0.685	2.24	1.98
	1.00	p(1 × 1)	−0.798	−0.553	NA	2.34	1.90
In_2O_3(110)	0.125	p(1 × 1)	−0.804	−1.239		2.27	2.04
	0.25	p(1 × 1)		−1.257			2.04
	0.50	p(1 × 1)		−1.188			2.04
	1.00	p(1 × 1)		−1.082			2.06

[a] Subscripts (H_2O, H−OH, Mixed) denote molecular, dissociated, and partial dissociation states of water adsorption, respectively. Bond lengths (in Å) between O of water and surface metal atom M (M = Ti, Sn, and In) in molecular adsorption (m_{O-M}) and dissociative adsorption (d_{O-M}) are shown in the last two columns.

To understand the markedly contrasting trends, we should first look at the electronic structure of water covered surfaces. These are shown in Figure 3 for the three oxide surfaces at the 1.0 ML coverage, i.e., one water molecule per surface metal atom. On SnO_2(110), the most dramatic effect upon dissociated water adsorption is a large downshift of the surface O 2p level toward the valence band. Comparing Figures 1a and 3a, the cog of the surface O 2p level is downshifted by as much as 1.20 eV. Similarly, on In_2O_3(110), the cog of the surface O 2p level is downshifted by 0.41 eV upon dissociated water adsorption (Figure 3b). The large downshifts indicate substantial energy gains upon water dissociation on the surface, and these numbers are much bigger than the hydrogen bond energies on the surface (typically less than 0.2 eV) or dissociation energy barriers (much less than 0.2 eV) on the surface.[9,20] By contrast, the movement of the surface O 2p level for *r*-TiO_2(110) (compare Figures 1c and 3c) is much more moderate, as there is almost no shift in its cog upon water

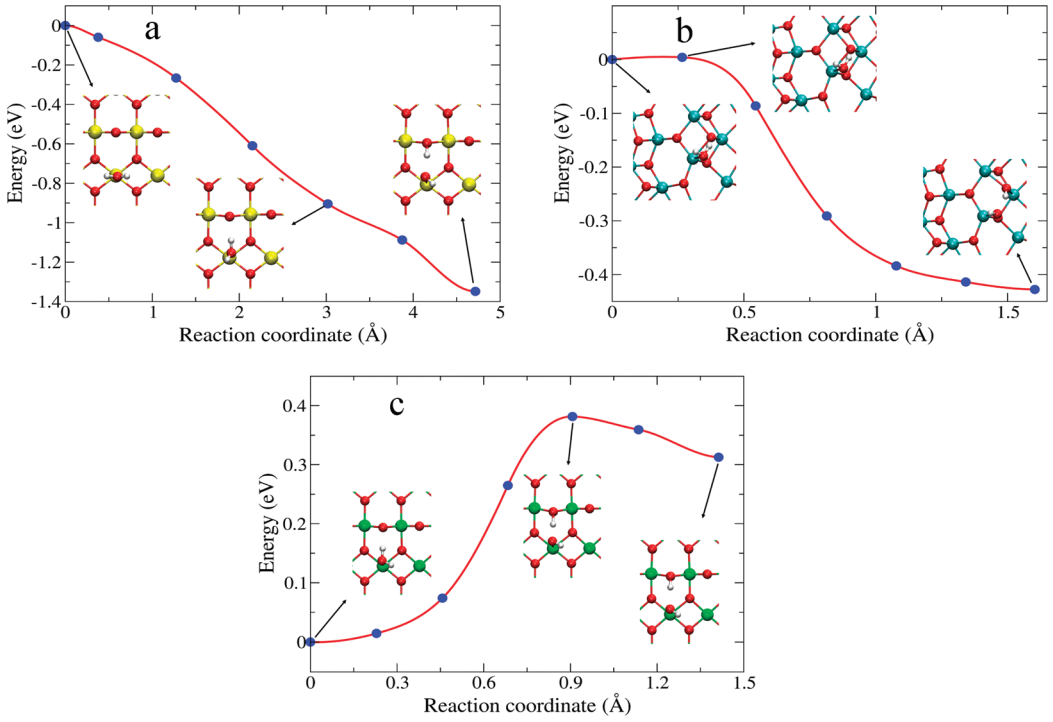

Figure 2. Potential energy profiles for water dissociation on oxide surfaces for (a) an isolated water molecule far away from the surface dissociates on a p(2 × 2) SnO_2(110) surface, (b) the transformation of a water molecule from molecular form to dissociated form on a p(1 × 1) In_2O_3(110) surface, and (c) the transformation of a water molecule from molecular form to dissociated form on a p(2 × 2) *r*-TiO_2(110) surface. The red, yellow, cyan, green, and white spheres represent O, Sn, In, Ti, and H atoms, respectively.

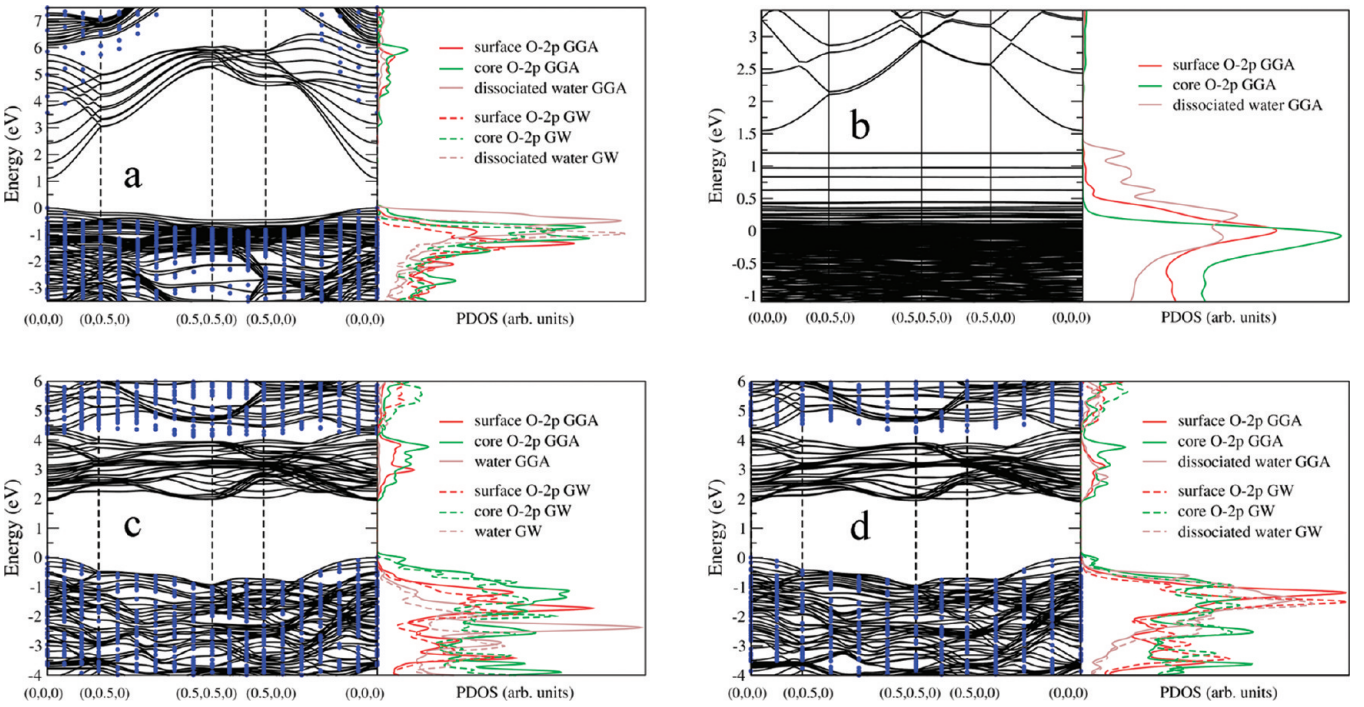

Figure 3. Electronic structure and PDOS of (a) dissociated water on $SnO_2(110)$ surface, (b) dissociated water on $In_2O_3(110)$ surface, (c) molecular water on *r*-$TiO_2(110)$ surface, and (d) dissociated water on *r*-$TiO_2(110)$ surface. Solid lines: DFT-GGA; dots and broken lines: GW. The top of bulk valence bands at Γ for DFT-GGA and GW results are set at zero.

Table 2. Bader CT σ Per Water (Unit in $|e|$) from Molecular or Dissociated Water to Oxide Surfaces at Different Coverages θ[a]

surface	θ	unit cell	σ_{H_2O}	σ_{H-OH}	σ_{Mixed}
$SnO_2(110)$	0.25	p(2 × 2)		0.05	
	0.50	p(2 × 1)		0.05	
	1.00	p(1 × 1)		0.04	
r-$TiO_2(110)$	0.083	p(6 × 2)	0.05	0.16	
	0.125	p(4 × 2)	0.05	0.15	
	0.25	p(2 × 2)	0.05	0.13	
	0.25	p(1 × 4)	0.03	0.10	
	0.333	p(1 × 3)	0.03	0.10	
	0.50	p(1 × 2)	0.03	0.10	
	0.50	p(2 × 1)	0.04	0.09	
	1.00	p(2 × 1)	NA	NA	0.04
	1.00	p(1 × 1)	0.03	0.09	NA
$In_2O_3(110)$	0.125	p(1 × 1)	0.03	0.04	
	0.25	p(1 × 1)		0.03	
	0.50	p(1 × 1)		0.04	
	1.00	p(1 × 1)		0.02	

[a] Subscripts (H_2O, H−OH, Mixed) denote molecular, dissociated, and partial dissociation states of water adsorption, respectively.

adsorption. It is useful to realize that the O 2p level of an adsorbed molecular water lies *below* the O 2p level of an adsorbed OH group (compare panels c and d of Figure 3). Therefore, as far as the water molecule *itself* is concerned, adsorption in molecular form has lower energy than the dissociated form. However, for an oxide whose surface O 2p level is in the band gap, then water in dissociated form can attach an H atom to a surface oxygen atom, forming an O_s−H bond. The formation of the O_s−H bond greatly reduces the energy of the O 2p level, as we have seen in $SnO_2(110)$ and $In_2O_3(110)$. This large energy gain drives the dissociation of water on these surfaces, making them effective water splitting agents. On the other hand, if the O 2p level is buried in the valence band, as in *r*-$TiO_2(110)$, the energy shift is much more moderate because of the dispersive nature of the surface O 2*p* states within the valence band, and water is likely to remain in molecular form, unless there are strong hydrogen bond interactions (see below).

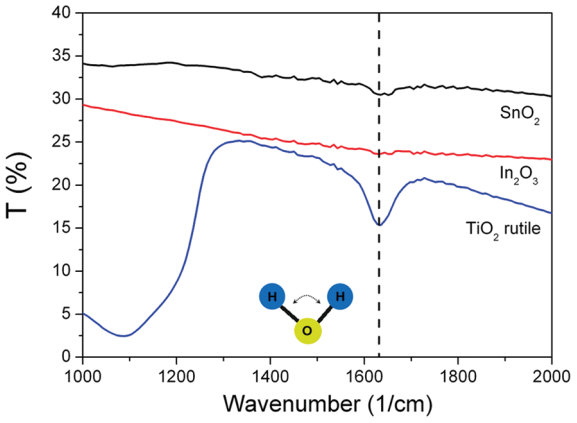

Figure 4. FTIR spectra for three oxide nanoparticles. The dashed vertical line marks the molecular water scissoring mode.

Another effect requiring investigation is the amount of charge transfer (CT) between the adsorbate and surface. CT processes may delete electrons from bonding molecular orbitals of water, weakening the O−H bonds, and finally producing dissociation. CT effects have been found to be important in water dissociation

dx.doi.org/10.1021/jp2032884 |*J. Phys. Chem. C* 2011, 115, 19710–19715

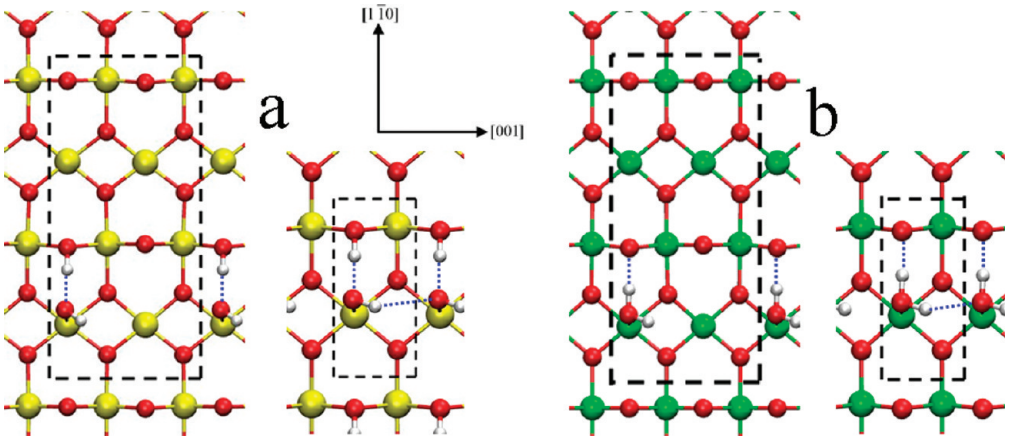

Figure 5. Top views of (a) dissociated water on $SnO_2(110)$ surface and (b) molecular water on *r*-$TiO_2(110)$ surface at low and high coverages. The red, yellow, green, and white spheres represent O, Sn, Ti, and H atoms, respectively. The blue dotted lines indicate hydrogen bonds.

in transition metal (TM)−(H_2O) systems.[30−32] We have carefully studied CT effects on water−metal oxide surfaces using the grid-based Bader scheme.[33] The calculated Bader charges are listed in Table 2. Contrary to the situation found in TM−(H_2O) systems, we find that CT effects are very small between either molecular water or dissociated water with metal oxide surfaces. For example, the CT between molecular water and the $TiO_2(110)$ surface is less than 0.06 e per molecule; for dissociated water on $SnO_2(110)$ and $In_2O_3(110)$ surfaces, the total CT between the dissociated species (dissociated OH + dissociated H) and the oxide surfaces is also less than 0.06 e. Thus, different than the situation of CT weakening O−H bonds leading to dissociation in TM−(H_2O) systems, there is little CT in metal oxide−(H_2O) systems. The most important factor deciding whether water dissociates or not on a metal oxide's surface remains the position of the surface O 2p level relative to the VBM.

To verify this conjecture, we carried out FTIR experiments to look for the presence of molecular water on the surface. According to our hypothesis, we expect to find little or no molecular water on either $SnO_2(110)$ or $In_2O_3(110)$, while we expect to find abundant molecular water on the *r*-$TiO_2(110)$ surface. The FTIR measurements are done under ambient conditions on nanoparticles of the three oxides. While the nanoparticles contain other surface facets, $SnO_2(110)$, $In_2O_3(110)$, and *r*-$TiO_2(110)$ are the dominant facets for each oxide. The dominant facets usually occupy more than 80% of the total surface area of metal oxide nanoparticles,[34−36] and in some cases dominant facets can occupy more than 90% of total surface area of metal oxide nanoparticles.[37,38] The measured FTIR spectra are shown in Figure 4 for the three oxides. The peak unique to molecular water vibration (the so-called water scissoring mode[39−41]) is at ∼1635 cm^{-1}. This peak can be used to characterize the presence of molecular water on a surface because it is easily distinguishable from various O−H stretching modes. From the data of Figure 4, the scissoring mode at ∼1635 cm^{-1} is very strong for rutile TiO_2 nanoparticles and almost nonexistent for either SnO_2 or In_2O_3 nanoparticles, exactly as predicted by theory.

In addition to the movement of the surface O 2p level, intermolecular interactions among neighboring water molecules/OH complexes or hydrogen bonds formed between a water molecule/OH complex and nearby surface oxygen can contribute to the total energy and hence to water dissociation. Intermolecular interactions include repulsive H−H and attractive H−O forces, and these forces are automatically included in the ab initio DFT calculations. Looking at the numbers in Table 1, the difference in adsorption energy per water molecule for $SnO_2(110)$ between 25% and full coverage is less than 0.05 eV. Although at full coverage, there is an additional hydrogen bond (bond length 2.45 Å) compared to the 25% case (see Figure 5a, blue dotted lines indicate hydrogen bonds), the energy difference is much smaller than the energy gained due to the downshift of the surface O 2p level. Therefore, hydrogen bond interactions are not the dominant forces driving water to dissociate on the surface of $SnO_2(110)$. Similarly, on $In_2O_3(110)$, the numbers in Table 1 show that the difference in adsorption energy per water molecule between 12.5% and full coverages is less than 0.16 eV, much smaller than the energy gained due to the downshift of its surface O 2p level. On the other hand, for *r*-$TiO_2(110)$, Table 1 shows that the difference in adsorption energy per molecule between molecular adsorption at p(2 × 2) and p(1 × 1) coverages is 0.09 eV. Assuming that this energy difference comes entirely from the additional hydrogen bond (bond length 2.12 Å, see Figure 5b, blue dotted lines), this magnitude is comparable to that between different forms of water adsorption (e.g., 0.113 eV at 1.0 ML between molecular and mixed forms). Thus, on oxide surfaces whose surface O 2p level does not appear in the band gap, hydrogen bond interactions are of a magnitude that can be important in water dissociation. Although our DFT calculations indicate that molecular water adsorption is preferred at all coverages on *r*-$TiO_2(110)$ (a result consistent with most recent experimental and theoretical findings[8,12]), the small energy differences of order 0.2 to 0.3 eV at many coverages between molecular and dissociative forms explain why this question remains controversial and under debate.

4. CONCLUSION

In summary, we have identified a class of metal oxide surfaces that are very effective in dissociating water. These oxide surfaces are characterized by having their surface O 2p level lying in the band gap and high above the VBM. Results of DFT-GGA and GW calculations and FTIR measurements support the notion that dissociated water can produce a large downshift of the surface O 2p level by attaching an H atom to the surface oxygen. As these oxide surfaces are effective water splitters, by the same token, they should

be effective in splitting other forms of hydrogen compounds. By contrast, metal oxide surfaces whose surface O 2p level is buried inside the valence band are less reactive to water and other hydrogen compounds, and on r-TiO_2(110), water adsorbs in molecular form at all coverages. The less reactive nature of r-TiO_2(110) and a-TiO_2(110) surfaces[20] due to the position of their surface O 2p level could explain why these surfaces make good electrodes in dye-sensitized solar cells (DSSCs)[42] because energy levels inside the band gap are less perturbed upon adsorption.

■ ASSOCIATED CONTENT

Supporting Information. The reaction pathway coordinates of the studied oxide surfaces. This material is available free of charge via the Internet at http://pubs.acs.org.

■ AUTHOR INFORMATION

Corresponding Author
*E-mail: tongsy@sustc.edu.cn.

■ ACKNOWLEDGMENT

The work described in this paper is supported by project RGC CRF CityU6/CRF/08 and RGC GRF HKU 701910. We thank the SCCAS, ACIM of the City University of Hong Kong, and the HPCCC of Hong Kong Baptist University for computational facilities.

■ REFERENCES

(1) Fujishima, A.; Honda, K. *Nature* **1972**, *238*, 37–38.
(2) Pang, C. L.; Lindsay, R.; Thornton, G. *Chem. Soc. Rev.* **2008**, *37*, 2328–2353.
(3) Fujishima, A.; Zhang, X. T.; Tryk, D. A. *Surf. Sci. Rep.* **2008**, *63*, 515–582.
(4) Chen, X. B.; Mao, S. S. *Chem. Rev.* **2007**, *107*, 2891–2959.
(5) Verdaguer, A.; Sacha, G. M.; Bluhm, H.; Salmeron, M. *Chem. Rev.* **2006**, *106*, 1478–1510.
(6) Diebold, U. *Surf. Sci. Rep.* **2003**, *48*, 53–229.
(7) Dulub, O.; Meyer, B.; Diebold, U. *Phys. Rev. Lett.* **2005**, *95*, 136101.
(8) Harris, L. A.; Quong, A. A. *Phys. Rev. Lett.* **2004**, *93*, 086105.
(9) He, Y. B.; Tilocca, A.; Dulub, O.; Selloni, A.; Diebold, U. *Nat. Mater.* **2009**, *8*, 585–589.
(10) Meyer, B.; Marx, D.; Dulub, O.; Diebold, U.; Kunat, M.; Langenberg, D.; Wöll, C. *Angew. Chem., Int. Ed.* **2004**, *43*, 6641–6645.
(11) Eng, P. J.; Newville, M.; Brown, G. E., Jr.; Waychunas, G. A. *Science* **2000**, *288*, 1029–1033.
(12) Allegretti, F.; O'Brien, S.; Polcik, M.; Sayago, D. I.; Woodruff, D. P. *Phys. Rev. Lett.* **2005**, *95*, 226104.
(13) Ferry, D.; Glebov, A.; Senz, V.; Suzanne, J.; Toennies, J. P.; Weiss, H. *J. Chem. Phys.* **1996**, *105*, 1697–1701.
(14) Giordano, L.; Goniakowski, J.; Suzanne, J. *Phys. Rev. Lett.* **1998**, *81*, 1271–1273.
(15) Lindan, P. J. D. *Chem. Phys. Lett.* **2000**, *328*, 325–329.
(16) Hass, K. C.; Schneider, W. F.; Curioni, A.; Andreoni, W. *Science* **1998**, *282*, 265–268.
(17) Vittadini, A.; Selloni, A.; Rotzinger, F. P.; Grätzel, M. *Phys. Rev. Lett.* **1998**, *81*, 2954–2957.
(18) Mulakaluri, N.; Pentcheva, R.; Wieland, M.; Moritz, W.; Scheffler, M. *Phys. Rev. Lett.* **2009**, *103*, 176102.
(19) Xu, H.; Zhang, R. Q.; Tong, S. Y. *Phys. Rev. B* **2010**, *82*, 155326.
(20) Xu, H.; Zhang, R. Q.; Ng, A. M. C.; Djurišić; A. B.; Chan, H. T.; Chan, W. K.; Tong, S. Y. to be published.
(21) Kresse, G.; Joubert, D. *Phys. Rev. B* **1999**, *59*, 1758–1775.
(22) Kresse, G.; Furthmüller, J. *Phys. Rev. B* **1996**, *54*, 11169–11186.
(23) Blöchl, P. E. *Phys. Rev. B* **1994**, *50*, 17953–17979.
(24) Perdew, J. P.; Wang, Y. *Phys. Rev. B* **1992**, *45*, 13244–13249.
(25) Thierfelder, C.; Hermann, A.; Schwerdtfeger, P.; Schmidt, W. G. *Phys. Rev. B* **2006**, *74*, 045422.
(26) Monkhorst, H. J.; Pack, J. D. *Phys. Rev. B* **1976**, *13*, 5188–5192.
(27) Henkelman, G.; Uberuaga, B. P.; Jónsson, H. *J. Chem. Phys.* **2000**, *113*, 9901.
(28) Hedin, L. *Phys. Rev.* **1965**, *139*, A796–A823.
(29) Liu, L. M.; Zhang, C. J.; Thornton, G.; Michaelides, A. *Phys. Rev. B* **2010**, *82*, 161415.
(30) Walters, R. S.; Pillai, E. D.; Duncan, M. A. *J. Am. Chem. Soc.* **2005**, *127*, 16599–16610.
(31) Bustamante, M.; Valencia, I.; Castro, M. *J. Phys. Chem. A* **2011**, *115*, 4115–4134.
(32) Stace, A. J.; Walker, N. R.; Firth, S. *J. Am. Chem. Soc.* **1997**, *119*, 10239–10240.
(33) Tang, W.; Sanville, E.; Henkelman *J. Phys.: Condens. Matter* **2009**, *21*, 084204.
(34) Batzill, M.; Katsiev, K.; Burst, J. M.; Diebold, U. *Phys. Rev. B* **2005**, *72*, 165414.
(35) Han, X. G.; Jin, M. S.; Xie, S. F.; Kuang, Q.; Jiang, Z. Y.; Jiang, Y. Q.; Xie, Z. X.; Zheng, L. S. *Angew. Chem., Int. Ed.* **2009**, *48*, 9180–9183.
(36) Ohno, T.; Sarukawa, K.; Matsumura, M. *New J. Chem.* **2002**, *26*, 1167–1170.
(37) Lazzeri, M.; Vittadina, A.; Selloni, A. *Phys. Rev. B* **2001**, *63*, 155409.
(38) Yang, H. G.; Sun, C. H.; Qiao, S. Z.; Zou, J.; Liu, G.; Smith, S. C.; Cheng, H. M.; Lu, G. Q. *Nature* **2008**, *453*, 638–641.
(39) Noei, H.; Qiu, H. S.; Wang, Y. M.; Löffler, E.; Wöll, C.; Muhler, M. *Phys. Chem. Chem. Phys.* **2008**, *10*, 7092–7097.
(40) Finnie, K. S.; Cassidy, D. J.; Bartlett, J. R.; Woolfrey, J. L. *Langmuir* **2001**, *17*, 816–820.
(41) Armaroli, T.; Busca, G.; Milella, F.; Bregani, F.; Toledo, G. P.; Nastro, A.; De Luca, P.; Bagnasco, G.; Turco, M. *J. Mater. Chem.* **2000**, *10*, 1699–1705.
(42) O'Regan, B; Grätzel, M. *Nature* **1991**, *353*, 737–740.